Fracture and bedding plane control on groundwater flow in a chalk aquitard

Menachem Weiss · Yoram Rubin · Eilon Adar · Ronit Nativ

Abstract Shallow groundwater in the northern Negev desert of Israel flows preferentially through a complex system of discontinuities. These discontinuities intersect what would otherwise be a massive, low-conductivity, high-porosity Eocene chalk. Vertical fractures and horizontal bedding planes were observed and mapped along approximately 1,200 m of scanline, 600 m of core and 30 two-dimensional trace planes. A bimodal distribution of size exists for the vertical fractures which occur as both single-layer fractures and multi-layer fractures. A bimodal distribution of log transmissivity was observed from slug tests conducted in packed-off, vertical intervals within the saturated zone. The different flow characteristics between the horizontal bedding planes and vertical-type fractures appear to be the cause of the bimodality. Two distinct conceptual models (discrete fracture network) were developed based on the fracture orientation, size, intensity and transmissivity statistics derived from field data. A correlation between fracture size and hydraulic aperture was established as the basis for calibrating the simulated model transmissivity to the field observations. This method of defining transmissivity statistically based on prior information is shown to be a reasonable and workable alternative to the usual conjecture approach towards defining transmissivity in a fractured-rock environment.

Résumé Les eaux souterraines phréatiques dans le Nord du désert de Néguev en Israël, s'écoulent préférentiellement à travers un système complexe de discontinuités. Ces discontinuités entrecoupent une craie Eocène massive, de faible conductivité et de haute porosité. Les fractures verticales et horizontales et les plans horizontaux stratifiés ont été observés et cartographiés sur approximativement 1,200 m de coupes, 600 m de carottes, et 30 plans en deux dimensions. Une distribution bimodale de la taille des fractures verticales a été observée. Ces fractures apparaissent comme de simples couches de fractures ou comme des fractures multi-couches. Une distribution bimodale de la transmissivité a également été observée à partir des résultats de slug tests réalisés en « packed off» sur des intervalles verticaux de la zone saturée. Les caractéristiques des différents écoulements entre les plans stratifiés horizontaux et les fractures verticales apparaissent comme la cause de cette bimodalité. Deux modèles conceptuels distincts (réseau de fractures discrètes) ont été développés sur base de l'orientation des fractures, leur taille, l'intensité et les statistiques de leur transmissivité dérivées des données de terrain. Une corrélation entre la taille des fractures et l'ouverture hydraulique a été définie comme le fondement de la calibration du modèle de la transmissivité sur les observations de terrain. Cette définition de la transmissivité statistiquement basée sur l'information précédente est présentée comme une alternative raisonnable aux approches usuelles visant à définir la transmissivité dans un environnement de roches fracturées.

Resumen El agua subterránea somera en el norte del desierto de Negev de Israel fluye principalmente a través de un complejo sistema de discontinuidades. Estas discontinuidades interceptan lo que de otra manera sería una caliza masiva Eocena de alta porosidad y baja conductividad. Se observaron y cartografiaron fracturas verticales y planos de estratificación horizontales que se detectaron aproximadamente a lo largo de una línea de 1,200, 600 m de núcleo y 30 planos de traza en dos dimensiones. Existe una distribución bimodal de tamaño para las fracturas verticales las cuales ocurren ya sea como

Received: 29 August 2004 / Accepted: 21 February 2006
Published online: 24 June 2006

M. Weiss (✉)
Institute of Earth Sciences,
The Hebrew University,
Jerusalem, Israel
e-mail: weissm@agri.huji.ac.il

Y. Rubin
Department of Civil and Environmental Engineering,
University of California at Berkeley,
Berkeley, CA, USA

E. Adar
Jacob Blaustein Institute for Desert Research and Department of Geological and Environmental Sciences,
Ben Gurion University of the Negev,
Sde Boker, Israel

R. Nativ
Seagram Center for Soil and Water Sciences,
Faculty of Agricultural,
Food and Environmental Quality Sciences,
The Hebrew University of Jerusalem,
Rehovot, Israel

 DOI 10.1007/s10040-006-0039-y

fracturas en una sola capa y fractures en capas múltiples. Se observó una distribución bimodal de los valores de transmisividad transformados logarítmicamente provenientes de pruebas de golpeo realizadas en intervalos verticales empacados dentro de la zona de saturación. La causa de la bimodalidad parecen ser las diferentes características de flujo entre los planos horizontales de estratificación y las fracturas verticales. Dos distintos modelos conceptuales (redes de fracturas discretas) se han desarrollado en base a la orientación, tamaño, e intensidad de fracturas y las estadísticas de transmisividad provenientes de datos de campo. Se estableció una correlación entre el tamaño de la fractura y la apertura hidráulica como base para calibrar el modelo simulado de transmisividad con las observaciones de campo. Se muestra que el método de definir estadísticamente la transmisividad en base a información previa constituye una alternativa razonable y trabajable al enfoque normal de conjeturas en la búsqueda por definir la transmisividad en un ambiente de roca fracturada.

Keywords Groundwater · Fractures · Chalk · Israel · Modeling · Geostatistics

Introduction

Fractures create a unique flow problem in that hydraulic conductivity variations are extreme and localized and the discontinuities are typically large in comparison to boreholes and measurement devices (Long et al. 1998). Because of the complex nature of these systems, and inadequate investigative techniques which often rely on extrapolating exposed features and indirect measurements, statistical network models have been adapted to characterize the discontinuous rock system (Odling 1997). To statistically model a three-dimensional flow system, fractures must be spatially characterized with respect to orientation, intensity (total area of fractures/total volume), size and aperture (or transmissivity; LaPointe and Hudson 1985). The interconnections of these fractures must also be characterized to understand the flow field (Long et al. 1998). Identifying the spatial distribution of fractures is difficult because of the chaotic and sometimes multiple nature of the geologic processes leading to their development.

The extreme heterogeneity existing in fractured aquifers has motivated many researchers to use statistics to help characterize the transmissivity distribution (e.g. Rubin 2002). Cacas et al. (1990), Tsang et al. (1996) and Seong and Rubin (University of California at Berkeley, 1998, personal communication) even considered bivariate statistics to help model the correlation structure of the heterogeneous conductivity field. Because flow in fractured rock is highly dependent on the variable aperture of the fracture plane, much effort has focused on understanding aperture geometry (Silliman 1989; Stratford et al. 1990; Cady et al. 1993; Dijk et al. 1999). Zimmerman et al. (1998) summarized the most popular inverse techniques for identifying aquifer transmissivity in fractured rocks.

Researchers have shown that the distributions of fracture length and aperture can be statistically correlated on the basis of qualitative and quantitative geological arguments (Odling 1993). The definition of fracture size in terms of statistical moments has often been discussed and the works of Villaescusa and Brown (1992), Mauldon (1998), Zhang and Einstein (1998), and Odling et al. (1999) are notable sources. It has been shown in a two-dimensional flow model that if aperture and length are correlated, the predicted global hydraulic conductivity is one order of magnitude greater than that in the uncorrelated case (Odling 1993). A linear relationship has been used to describe the correlation between fracture aperture and length for single, isolated veins in extensional fractures (Stone 1984; Vermilye and Scholz 1995). For more complex, natural fracture systems, a power-law correlation has been identified that appears to be influenced by interactions with neighbouring fractures (Hatton et al. 1994; Vermilye and Scholz 1995; Johnston and McCaffrey 1996; Renshaw and Park 1997). Further studies have shown that a certain characteristic length scale, the point at which interaction effects caused by increasing fracture density begin to influence the correlation coefficients, may be quantifiable (Main et al. 1999). Walmann et al. (1996) showed how a non-linear relationship between fracture size and aperture is evident in laboratory deformation experiments. Such relationships make good geophysical sense when the apertures under consideration are undisturbed. However, in nature, secondary effects of dissolution, chemical action, fault-gouge development and/or normal pressures caused by overburden can obliterate any underlying size-aperture relationships (Stone 1984; Bonnet et al. 2001). Stone (1984) noted that since fracture cross sections are elliptical, aperture data is biased with respect to measurement location. A complete aperture survey of each fracture is therefore important.

The objective of this study was to characterize the geometrical parameters defining the variation of the fracture network in space, and assess their control on groundwater flow at a field site underlain by highly porous, fractured chalk. A statistical method, which utilizes a correlation between fracture size and fracture aperture, was used to define transmissivity in a discrete fracture network (DFN) model. The transmissivity data derived from the fracture data were used with two alternative groundwater flow models, potentially appropriate for the hydrogeological setting of the study area, and calibrated against transient flow conditions (aquifer slug tests). Most fracture flow studies have focused on plutonic- and metamorphic-type rocks which have much less matrix permeability than the chalk in question. Furthermore, very few (if any) models have been presented in the literature which actually show how a correlation between fracture length and aperture can be useful for defining the ever-elusive transmissivity parameter.

 DOI 10.1007/s10040-006-0039-y

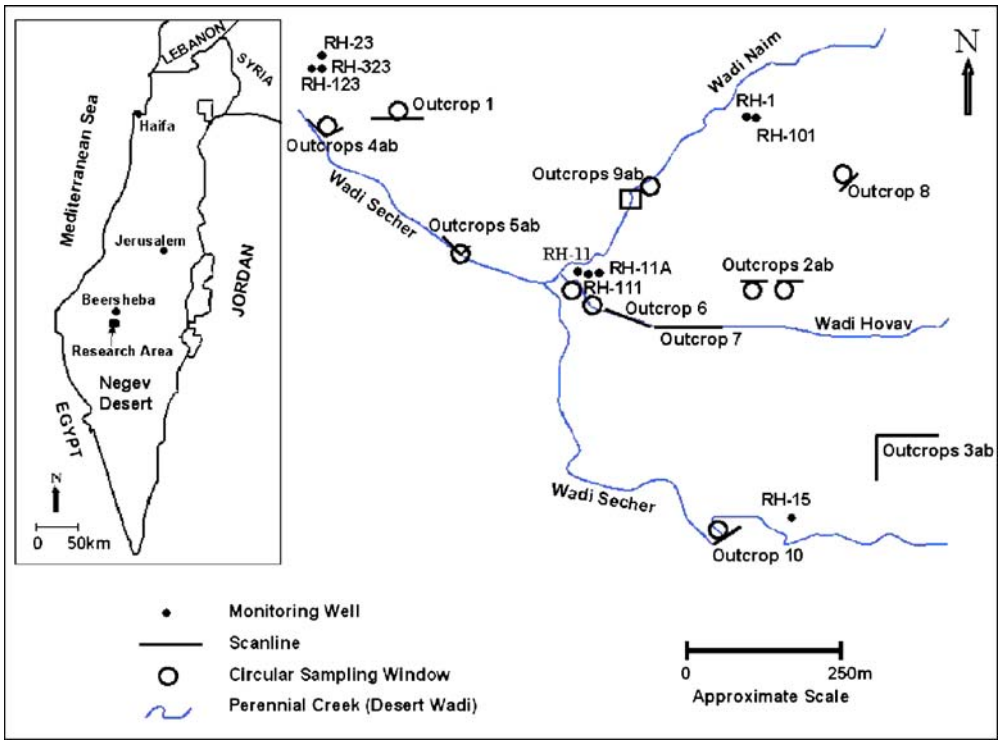

Fig. 1 Map of Israel, West Bank, Golan Heights, Gaza Strip and adjacent countries, and site map showing the research area and three major perennial streams, outcrop locations, and monitoring locations

Geology and hydrology at the field site

The study area is located within the Ramat Hovav Industrial Complex, in the northern Negev desert, Israel (Fig. 1). This complex is underlain by fractured, porous chalk, the thickness of which ranges from 150 to 285 m. Groundwater contamination has been caused through wastewater release and leakage from the various plants and wastewater treatment and storage facilities on site. It was once thought that the site was ideal for prohibiting migration of contaminants from the surface to groundwater because of the arid climatic conditions and because the rocks provided a natural geological barrier. It is now clear, however, that the chalk underlying the area allows for relatively rapid transport of contaminants from the surface to the groundwater flow system via the vertical joint sets, horizontal bedding planes and dissolution channels (Nativ and Nissim 1992; Rophe et al. 1992; Nativ et al. 1995, 1999).

The site is located in one of the many NE–SE trending synclines of the arid northern Negev. The uppermost chalk formations have been fractured by different mechanisms, including burial, syntectonic uplift and post-uplift processes (Bahat 1991), to create a relatively systematic pattern of vertical joint sets, classified into single-layer and multi-layer types. Fractures belonging to the burial-mechanism class were formed relatively soon after the original rock induration and are observed in the field as single-layer joints with relatively small spacings. Whereas the apertures of uplift joints are wide and decrease with depth, those of the burial joints increase with depth since they have a historical genesis of advancing upwards (Bahat 1999). Fractures formed by uplift, although observed mainly as multi-layer with much larger spacings, can also occur as single-layer joints.

Bahat and Adar (1993) and Nativ et al. (1999) concluded that groundwater flow on site is primarily controlled by the N55-60E joint system. Bahat and Shavit (1997) suggested that although the relatively horizontal bedding planes intersected by the NNW–NNE-oriented vertical joints probably provide a secondary hydraulic connection, the main subsurface flow is controlled by the N62E multi-layer vertical fractures that parallel the major fold axes.

A number of artificially exposed outcrops exist at the site (Fig. 2a) to study the relationship between groundwater flow and rock discontinuities (joints, fractures and bedding planes). In addition, as part of this study, trenches were dug into the saturated chalk below the water table providing unique, direct exposure of groundwater seeping out of the fractures into the chalk (Fig. 2b). The trenches were dug to a maximum depth of approximately 3 m, and some were hundreds of meters in length. A number of boreholes were also drilled at the site and the retrieved cores were analysed for fracture statistics and morphology.

Correlation between fracture size and hydraulic aperture

The following relationship accounts for either a linear or non-linear correlation between a fracture's measured aperture (b) and size (L):

$$b = C_1 L^{C_2} \quad (1)$$

 DOI 10.1007/s10040-006-0039-y

Fig. 2 **a** Typical vertical outcrop (approximately 4 m high) showing bedding planes and both single-layer and multi-layer vertical discontinuities. **b** A portion of the 475-m long, ~2–5 m-deep trench dug into the saturated chalk

where C_1 and C_2 are the correlation coefficients. Depending upon how one conceptualizes the three-dimensional geometry of a fracture, the size term (L) in the above equation may refer to either the length and/or width of a rectangular-shaped fracture, or the diameter of a circular-shaped fracture. Table 1 contains the C_1 and C_2 coefficient values found from a literature survey for studies describing the relationship between measured fracture apertures and measured fracture lengths. If Eq. 1 is combined with the cubic law, describing flow through a fracture, the relationship between the effective hydraulic transmissivity (T_e) and fracture size is obtained:

$$T_e = \left(C_1^2 L^{2C_2}\right) \times \frac{g}{12\nu} \times L \qquad (2)$$

where g is the acceleration of gravity and ν is kinematic viscosity. It is important to understand that the relationship in Eq. 2 assumes that the relationship shown in Eq. 1 is consistent for the effective hydraulic aperture as well as the measured aperture. The effective hydraulic aperture may be significantly less than the measured aperture due to a number of reasons including uneven fracture wall topography and mineralization on the fracture wall surface. Plenty of research papers have been devoted to understanding the relationship between the two apertures and the reader is referred to Silliman (1989), Tsang (1992) and Weisbrod et al. (1998) for more information.

In this study, the representative populations of fracture sizes were identified from the field data, revealing a bimodal size distribution termed as either single-layer fractures or multi-layer fractures (Fig. 2a). However, although the single-layer and multi-layer fractures are easily distinguishable on sub-vertical outcrop exposures where bedding planes are exposed (Fig. 2a), on sub-horizontal exposures (along wadi channels) a sub-vertical fracture's relationship with the bedding planes is unknown. In this case, the fractures are termed either short-type or long-type, which is not always analogous to single-layer or multi-layer, respectively. This phenomenon became clear during the drilling of cores on a horizontal outcrop at the research site where it was observed that although drilling was executed into a particularly long and widely opened fracture, the fracture disappeared at a depth of less than a half-meter into the rock. Conversely, short fracture lengths observed on these exposures may actually be multi-layer fractures.

Given adequate estimates of the correlation parameters in Eq. 2, the resulting fracture size data should allow for an identification and characterization of the effective transmissivity. However, the assumption that measured aperture and effective hydraulic aperture are identical (or at least correlated in some definable way) may not be valid. Therefore, conclusions regarding the correlation between fracture length and transmissivity must be drawn with caution. In this study, the correlation-parameter values from Table 1 were used initially as a rough estimate and were then more clearly defined through a process of conditioning to actual transmissivity field data, as described further on.

Fracture size statistics

Because of the bimodal size distribution, the four fracture types (single, multiple, short and long) were analysed using different field techniques. Single-layer/short fractures were analysed using a circular sampling window technique (Zhang and Einstein 1998). The theory allows for a prediction of the mean trace length assuming planar fractures with uniformly distributed trace-length midpoints. The method is particularly effective in estimating the mean trace length without the effects of orientation bias and does not require knowledge of the trace length distribution. Three types of discontinuities intersect such a circular window: N_0 (both of the fracture ends extend outside the window bounds, i.e. complete censoring by the window), N_1 (one fracture end censored by the window) and N_2 (no ends censored by the window, i.e. both of the fracture ends exist within the window bounds). The total number of each type of fracture intersecting the window

 DOI 10.1007/s10040-006-0039-y

Table 1 Published data regarding fracture size-aperture correlation

Relationship formula	C_1 value	C_2 value	Data source
$b = L^{c_2}$	1	0.44–0.50	Laboratory deformation experiments on clay[a]
$b = L^{c_2}$	1	1.96–2.44 0.81–0.97	Tensile fractures in basalt fissure swarm, Iceland[b]
$b = L^{c_2}$	1	1.31–2.25 0.55–0.71	Tensile fractures in basalt fissure swarm, Iceland[b]
$b = L^{c_2}$	0.021	1.2	Quartz/gold vein fills in quartzite, Ireland; parallel section[c]
$b = L^{c_2}$	0.001	1.47	Quartz/Gold vein fills in quartzite, Ireland; perpendicular section[c]
$b = L^{c_2}$	0.023	1.08	Calcite veins in calcarenite and calcsilicates, Ireland; perpendicular to bedding[c]
$b = L^{c_2}$	0.018	0.99	Calcite veins in calcarenite and calcsilicates, Ireland; bedding planes[c]
$b = L^{c_2}$	0.002	1.2	Quartz veins in sandstone, Ireland; bedding planes[c]
$b = L^{c_2}$	0.016	0.95	Quartz veins in sandstone, Ireland; perpendicular to bedding[c]
$b = L^{c_2}$	0.01	1.15	Quartz/pyrite/galena veins in marble, Ireland; horizontal plane[c]
$b = L^{c_2}$	0.00002	1.49	Quartz veins in granite, Ireland; horizontal plane[c]
$b=C_1L$	0.0031	1	Single-segment, Quartz-filled fractures in orthoquartzite-pebble conglomerate, New York, USA[d]
$b=C_1L$	0.0082, 0.0073, 0.0031, 0.0044, 0.0033	1	Single-segment, Calcite and quartz-filled fractures in limestone and sandstone, Quebec, Canada[d]
$b=C_1L$	0.0015	1	Single-segment, calcite veins in a diabase dike, New York, USA[d]
$b=C_1L$	0.00077	1	Single-segment, calcite veins in layered argillite, New York and Vermont, USA[d]
$b=C_1L$	0.0025	1	Calcite, dolomite and quartz-filled fractures in limestone, Pennsylvania, USA[d]
$b=C_1L$	0.0034	1	Single-segment, calcite veins in calcareous siltstone, Virginia, USA[d]
$b=C_1L$	0.00032	1	Multi-segment, calcite veins in calcareous siltstone, Virginia, USA[d]
$b=C_1L^{0.5}$	0.03	0.5	Multi-segment, calcite veins in calcareous siltstone, Virginia, USA[d]
$b=C_1L$	0.0019	1	Single-segment, chlorite/epidote-filled fractures in granodiorite, California, USA[d]
$b=C_1L$	0.00021	1	Multi-segment, chlorite/epidote-filled fractures in granodiorite, California, USA[d]
$b=C_1L^{0.5}$	0.022	0.5	Multi-segment, chlorite/epidote-filled fractures in granodiorite, California, USA[d]
$b=C_1L$	0.001	1	Single-segment, numerical solutions based on elastic crack theory[e]
$b=C_1L^{0.5}$	0.0018	0.5	Multi-segment, Numerical solutions based on elastic crack theory[e]
$b=C_1L^{0.5}$	0.096	0.5	Multi-segment (250-mm lengths), calcite veins in calcareous siltstone, Virginia, USA[d]
$b=C_1L^{0.5}$	0.061	0.5	Multi-segment (100-mm lengths), calcite veins in calcareous siltstone, Virginia, USA[d]
$b=C_1L^{0.5}$	0.014	0.5	Multi-segment (5-mm lengths), calcite veins in calcareous siltstone, Virginia, USA[d]
$b=C_1L$	0.07	1	Epidote-filled fractures in granite, Ontario, Canada[f]
$b=C_1L$	0.052	1	Chlorite-filled fractures in granite, Ontario, Canada[f]
$b=C_1L$	0.146	1	Faults in granite, Ontario, Canada[f]

[a] Walmann et al. (1996)

[b] Hatton et al. (1994) and Main et al. (1999)

[c] Johnston and McCaffrey (1996) (requires units in millimeters)

[d] Vermilye and Scholz (1995)

[e] Polllard et al. (1982)

[f] Stone (1984)

b fracture aperture, L fracture length, C_1 and C_2 correlation coefficients

(N) is tabulated and the mean trace length, μ_L, is then calculated using the formula:

$$\mu_L = \frac{\pi(N + N_0 - N_2)}{2(N - N_0 + N_2)} R \tag{3}$$

where R equals the radius of the circular sampling window. Radii of 1.0, 1.5 and 2.0 m were drawn onto the chalk surface at nine different locations (Fig. 1).

One benefit of the circular sampling window technique is that it provides a large amount of data in a relatively short period of time from even the smallest outcrops, allowing for the analysis of regional trends. For instance, fractures observed along the Naim and Secher washes (Fig. 1) appear to be distinctly smaller (i.e. they have distinctly smaller diameters) than fractures in outcrops situated away from the washes. A major drawback of the circular sampling window technique is the physical limitation of drawing a large (two-dimensional) circle

 DOI 10.1007/s10040-006-0039-y

onto outcrops which are typically limited in their two-dimensional extent. This limitation precludes the use of the technique for analysis of particularly large fractures.

Information regarding the length of multi-layer/long-type fractures (along with the single-layer/short-type fractures) was derived from trace length measurements along more than 1,200 m of scanline and a two-dimensional trace plane. The latter was drawn directly onto a horizontal outcrop surface in the shape of a rectangle approximately 5 by 3 m. It was later digitized onto the computer for a detailed analysis. Most of the scanlines were taken from the base of sub-vertical man-made outcrops within the unsaturated zone of the chalk. Exceptions include scanlines from outcrops 4ab and 9ab, laid out along the top of sub-horizontal wadi channels, and outcrops 5ab, 6 and 7, created by digging trenches into the water table approximately 2 m below the surface at these locations (Fig. 1). Pumping of the accumulated groundwater in the trenches exposed chalk layers normally below the water table for mapping.

The data derived from these exercises were analysed using the FracSize computer program (Dershowitz et al. 1998) which simulates trace length sampling (taking into account censoring, truncation and sampling bias) to determine the appropriate distribution of fracture radii that best matches the observed data. Nearly all of the multi-layer fractures seen on vertical outcrops, and many of the distinctly long fractures exposed on the wadi floors, are censored by the extent of the outcrops, thereby allowing only a semi-trace length measurement to be obtained. The effects of censoring on data analysis have been well studied and a number of correction methods have been offered (Villaescusa and Brown 1992; Zhang and Einstein 1998). The truncation bias was directly dealt with by attempting to measure all visible discontinuities no matter how short. Priest and Hudson (1976) showed that data truncated at 1 cm (i.e. ignoring fractures less than 1 cm long) have only a small effect, particularly if the mean trace length is on the order of meters. The need to correct for the other sampling biases (orientation and size) has been described at length in the literature for many years (e.g. Terzaghi 1965; LaPointe and Hudson 1985). The trace length data for each fracture set from each outcrop was analysed separately to eliminate these biases as well as to describe the stationary nature of fracture size across the study area.

Results of the fracture-size analyses showed a lognormal size distribution to be the most appropriate. Assumption of a power-law model always produced a much lower Kolmogorov-Smirnov (K-S) statistical measure of goodness-of-fit. Although there are physical grounds for why discontinuity properties should follow power laws, the presence of a characteristic length scale in the system (single-layer fractures for example) can give rise to lognormal distributions that reflect reality (Odling et al. 1999; Bonnet et al. 2001). This does not, however, explain why the multi-layer fracture data tended more towards the lognormal distribution. One explanation is that the limited size of the data sets (usually less than 60 measurements) precluded the accurate estimation of a reliable power-law exponent. Bonnet et al. (2001) suggested that at least 200 measurements are needed to even begin to define the exponents of a power-law length distribution. The K-S percentage was usually low, which further suggests that the database was smaller than ideal.

Evidence of flow in fractures and bedding planes

Data regarding evidence of flow on discontinuity planes were recorded. However, in many cases it was impossible to get close enough to clearly examine the discontinuity planes. The criteria used as evidence of flow include black manganese or iron-red spots and stains, and fine to coarse gypsum mineralization. Since gypsum mineralization in an otherwise open discontinuity plane would tend to impede flow, it might seem more appropriate to classify this subset of discontinuities as "non-flowing" in the discrete fracture-flow model. However, gypsum was rarely found in cores: it appears to be a surface phenomenon and its effect on subsurface flow is therefore probably insignificant. The most meaningful data regarding flow was actually collected in the trenches dug below the water table. Seeping groundwater was observed in both the vertical fractures and horizontal bedding planes in the various trenches.

The total number of multi-layer fractures with evidence of past flow, and discontinuities with visual seepage, were tabulated separately. Of the 1505 discontinuities mapped across the site, 194 (12.9%) were either multi-layer with evidence of flow or showed actual seepage. Of these 194 "wet" fractures, approximately 42% were from the N60E set, approximately 47% were from the N30W set, and the remaining 21 were from other minor sets. The mean spacing of "wet" fractures belonging to the N30W and N60E fracture sets was 4.6 and 5.1 m, respectively.

Transmissivity data

Hydraulic conductivity values were obtained in the field through 60 slug tests, in packed-off 2- or 2.5-m-long intervals in eight boreholes (Assaf 2000; Kurtzman et al. 2003; for borehole location see Fig. 1). Although most intervals were pre-selected to include fractures previously observed in core and video logs of the borehole walls, some non-fractured sections were also tested to assess the conductivity of the chalk matrix. Because the chalk matrix at the site has extremely low hydraulic conductivity, the high values of calculated hydraulic conductivity are expected to represent the effective hydraulic conductivity of the discontinuities isolated within each packed-off interval. The Bouwer and Rice method (Bouwer and Rice 1976; Bouwer 1989) was used to analyse the field results and calculate the hydraulic conductivity values. There are a number of issues regarding the use of the Bouwer and Rice method to analyse packed intervals in a discontinuous rock envi-

 DOI 10.1007/s10040-006-0039-y

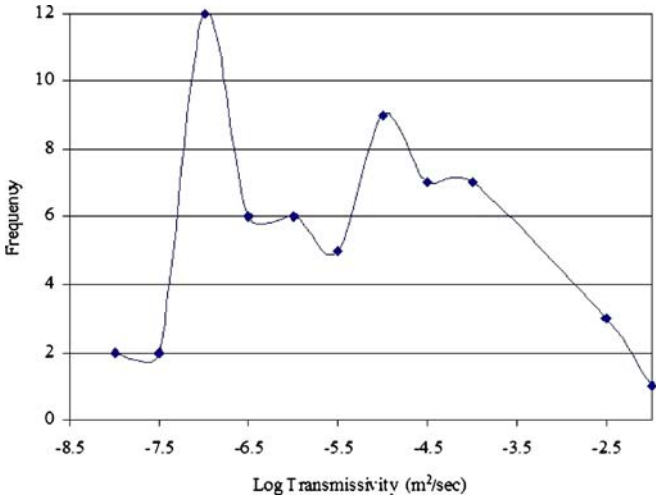

Fig. 3 Histogram of log-transmissivity values from 60 packer slug tests conducted in 2 or 2.5-m-long intervals of eight different boreholes in the study area

ronment which will not be elaborated upon here, rather, the reader is referred to Assaf (2000) for a complete discussion of the assumptions involved.

Figure 3 shows the resulting histogram of the 60 log-transmissivity values obtained from the packer slug tests. The data follows a bimodal trend of lognormality that is proposed here to be an artefact of the variation in transmissivity being provided by the bedding planes and the vertical fractures. A comparison of the slug-test results with the core logs, video logs, and subsequent detailed mapping of the cores revealed that in general, the highest hydraulic conductivity values are obtained where bedding planes intersect vertical fractures. Sections tested where only vertical fractures or only bedding planes are present show the lowest values of hydraulic conductivity. Due to the orientation of the tested boreholes (either vertical or slanted 20° from vertical with strike perpendicular to one of the major fracture sets), it is unclear whether the transmissivities resulting from the vertical fractures are representative of a single vertical fracture set or of an intersecting pair of vertical fractures (commonly seen in outcrops). Visual observations of flow in the trenches showed that whereas vertical fractures provide most of the flow, especially where two vertical fractures (conjugate set) bisect one another, horizontal bedding planes appear to contribute much less seepage. This latter observation was incorporated into the hydrologic models, by assuming that the vertical fractures are responsible for the higher transmissivity values while the bedding planes are responsible for the lower transmissivity values.

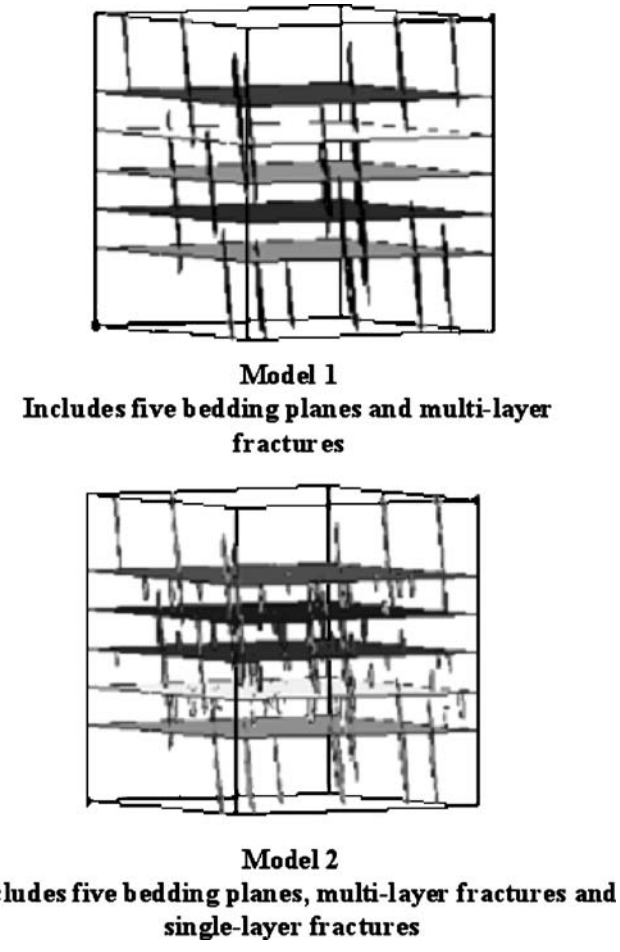

Fig. 4 Simplified view of the two conceptual models utilized in the discrete fracture network model

 DOI 10.1007/s10040-006-0039-y

Table 2 Information regarding the parameters utilized for generation of discrete fracture network

Fracture set	Model type	Mean pole-to-plane trend and plunge (degrees)	Fisher coefficient	P_{32} intensity (m^{-1})	Size distribution type	Mean and standard deviation of radii (m)	Transmissivity distribution
Multi-layer N30W	BART	239/1.0	26.4	0.138	Lognormal	5.15/1.28	Correlated with size
Multi-layer N60E	BART	149/3.1	31.1	0.076	Lognormal	3.1/0.44	Correlated with size
Beds	Single-fractures	0/90	5000	5 Beds	Constant	500	Constant
Single-layer N30W	BART	239/1.0	26.4	0.00138	Lognormal	0.42/0.64	Correlated with size
Single-layer N60E	BART	149/3.1	31.1	0.00076	Lognormal	0.25/0.21	Correlated with size

All fractures were generated as 6-sided polygons with an aspect ratio of 1. P_{32} refers to the areal intensity of fractures (total area of fractures per unit volume)

Conceptual model development

Because the single-layer fractures are relatively small (in both two-dimensional size and aperture), their importance as water conduits is unclear. Computational resources could be significantly freed up if the single-layer fractures could be ignored in the DFN flow model. On the other hand, these smaller fractures may play an important role in providing the needed connectivity to allow flow across the modelled region. Therefore, two separate conceptual models, one which includes both the multi-layer and single-layer fractures, and another which disregards the single-layer fractures, were defined. The different modelling results from each of the conceptual models provide important insight into how these apparently "minor" features influence the overall flow field. Figure 4 shows a schematic drawing of each of the conceptual models.

Based upon the statistical information obtained from the field surveys (orientation, intensity, length and transmissivity), two sets of vertical multi-layer fractures (models 1 and 2) and two sets of vertical single-layer fractures (model 2 only), as well as horizontal bedding planes (models 1 and 2), were simulated in a box region of 100 by 100 m with a depth of ~34 m using the FracWorks modelling software. The detailed characteristics of these models are provided in the following:

1. All fractures in the DFN were generated initially as planar, six-sided polygons with an aspect ratio of 1 (i.e. nearly circular discs). A fracture truncation algorithm (BART) based on a generalization of the Baecher discrete fracture model (Dershowitz et al. 1998) was used and allowed for some designated percentage of fracture centres to be generated from points on previously generated fractures. While the Baecher model is based upon generating fractures from centres located randomly in space (stationary Poisson-point process), the BART generalization allows for fracture truncation at only one possible intersection with an adjacent fracture, resulting in non-uniform fracture locations. Due to its ability to preserve the fracture size distribution, important for the applied size-transmissivity correlation, the BART conceptual model option was used invariantly in the generation of DFN models. All generated discontinuities were purposely not truncated at the generation region to avoid irregularities at the model boundaries.
2. Regarding orientation, all the fracture sets were designed to follow a Fisher distribution with a mean pole-to-plane trend and plunge value. In particular, the horizontal beds were given a Fisher parameter of 5,000 to account for the extreme consistency of bedding-plane orientations at the site.
3. Vertical-fracture intensity was input into the models based upon the spacing data obtained from the field surveys and the results of simulated sampling using a module included with the FracWorks software. This method produces a nearly three-dimensional approximation of the fracture intensity (total area of fractures/total volume) throughout the modelled region. Since many fractures within the overall population do not serve as flow conduits, it is reasonable to consider only a subset of the population when applying intensity to the DFN model (Chiles and de Marsily 1993). Consequently, the resulting values of intensity for the multi-layer fractures were decreased in both models to 20% to represent the percentage of fractures expected to provide flow. This percentage was based on visual observations in the trenches below groundwater and evidence of flow on the mapped outcrops. This process resulted in intensity values of 0.138 and 0.076 m^{-1} for the N30W and N60E multi-layer fracture sets, respectively. In model 2, the single-layer fracture intensity was decreased to 0.2% of the measured value, resulting in intensity values of 0.00138 and 0.00076 m^{-1} for the N30W and N60E sets, respectively. The different intensities used for the two fracture types is reasonable since the single-layer fractures are expected to contrib-

 DOI 10.1007/s10040-006-0039-y

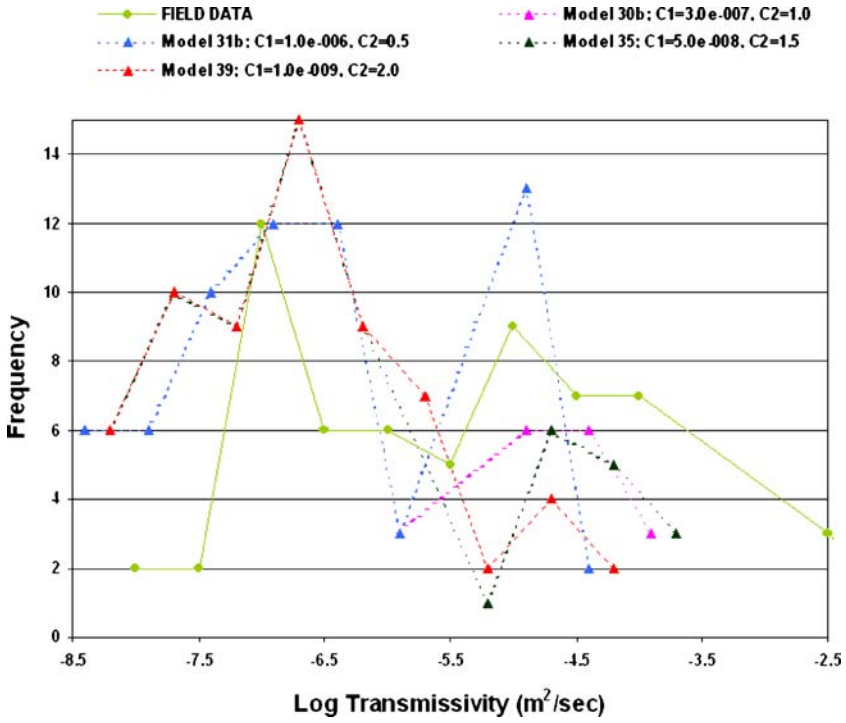

Fig. 5 Histogram of results from hydrotest simulations and slug-test field data

ute much less than the multi-layer fractures towards the overall flow.

4. The fracture size distribution for each set of vertical fractures was input as lognormal with mean and standard deviation values derived from the field-data statistics. For the horizontal bedding planes, size was input as a constant parameter, large enough to completely cover the 100 by 100 m model region.
5. Transmissivity was assigned to the vertical fractures according to a positive correlation with fracture size. Parameters C_1 and C_2 in Eq. 2 were initially chosen within the range shown in the literature (Table 1) and were subsequently modified iteratively in an attempt to calibrate the DFN model to the transient, slug-test field data. Bedding planes in the model were assigned transmissivity values deterministically according to a lognormal distribution with a mean and standard deviation of 1.37E-007 and 1.27E-007 m^2/s, respectively, based on calibration of the model to the best fit of the first peak in the bimodal lognormal distribution observed from the slug-test data.

Based on the above conceptual elements and statistical data for the DFN model, a groundwater flow model was subsequently developed to simulate flow through the generated network of fractures. Table 2 summarizes the details regarding orientation, intensity, size and other options for each of the fracture sets simulated in the flow model.

Numerical modelling attempts and slug-test simulation

The FracWorks software, which simulates flow through the generated network of interconnecting disks, was initially chosen to numerically model groundwater flow through the fractured chalk. A mesh-generation algorithm simplifies the overall DFN by calculating fracture intersections, and then fractures are discretized using finite triangular elements, assigning nodes to the resulting element mesh. This mesh can then be refined to accommodate boundary conditions such as pumping wells. Using a Galerkin finite-element solution (Dershowitz et al. 1998), the flow program approximates the diffusivity equation, describing two-dimensional flow. Simulation of pumping tests in the program involved generating internal boundary conditions within the flow field. An attempt was made to simulate the packer slug tests. However, it was determined early on that the model's algorithm could not accommodate the instantaneous change in head required for proper simulation. Therefore, an attempt was made to simulate long-term pumping tests, again resulting in the flow model's failure to discretize nodes satisfactorily at the sensitivity needed to analyse the transient response. Consequently, an alternative technique was utilized to analyse the transmissivity of simulated slug tests in the DFN modelling region as described below.

Twelve 30-m-long vertical wells were simulated at different lateral locations within the simulated DFN models, with each well broken into ten 3-m-long packer

 DOI 10.1007/s10040-006-0039-y

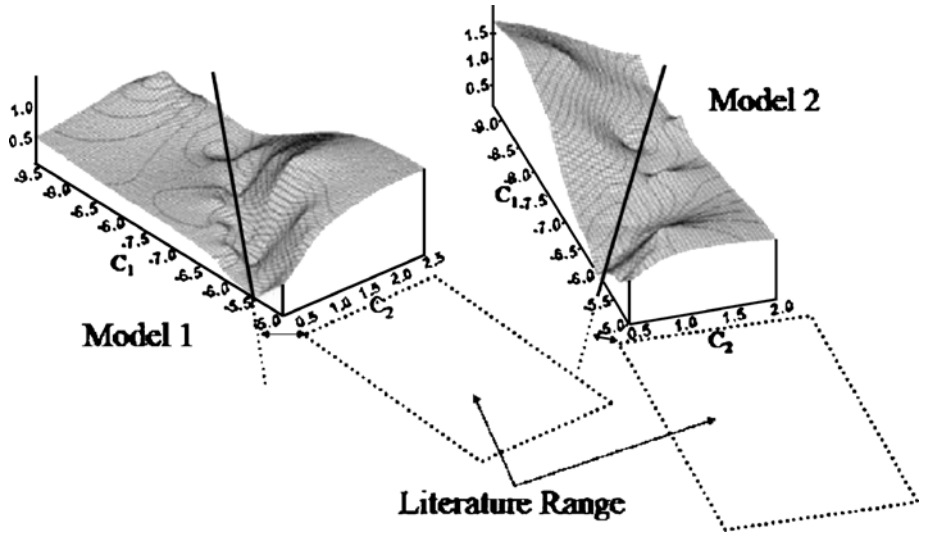

Fig. 6 Wireframe plots of mean transmissivity error as a function of C_1 and C_2 parameters

intervals. The transmissivity of each discontinuity intersecting the well was assumed to be a consequence of only that individual discontinuity without any contribution from secondary or more "feeder" discontinuities. This assumption closely mimics the actual field conditions since slug tests only displace a modest amount of water in the immediate vicinity of the boreholes tested. The net transmissivity of a test zone (packer interval) was calculated as the sum of the transmissivities of the conductive discontinuities that intersect that test zone according to the following equation:

$$T_i = \sum_{j=1}^{ni_i} T_{ij} \tag{4}$$

where T_i is the apparent transmissivity of the ith packer interval, n_i is the number of conductive discontinuities in the ith interval and T_{ij} is the transmissivity of the jth conductive discontinuity within the ith interval. Multiple realizations of DFN models with well simulations were generated to confirm the consistency of the results; each DFN simulation producing 120 transmissivity values.

Figure 5 shows a histogram of log-transmissivity results from the field data (shown also in Fig. 3) and four different DFN simulations (transmissivity computed on the basis of geometric relationships/correlations alone). Based on visual observations from the trench, which suggested that the vertical fractures have higher hydraulic conductivity than the horizontal bedding planes, the first histogram peak in each of the models was conditioned towards the transmissivity from the horizontal bedding planes while the second peak was conditioned towards the transmissivity of the vertical fractures. The four DFN models shown in the figure differ only with respect to the parameter values correlating size and transmissivity for the vertical fractures. The exponent correlation parameter value (C_2) was established as 0.5, 1.0, 1.5 or 2.0, and the coefficient value of C_1 was modified iteratively to obtain a close match to the field data. Throughout the simulations, the exponent (C_2) was established at many other values ranging between 0.25 and 2.5, in accordance with the published data regarding fracture length-aperture correlations (Table 1) indicating a C_2 parameter range between 0.44 to 2.44 and a C_1 parameter range between 2.0E-005 and 1.0. In the simulations, the values used for the C_1 parameter were below the literature range (1.0E-009–1.0E-006): this was necessary because simulations where C_1 had values at or over 1.0E-005 required C_2 values approaching (below) zero.

Another important parameter analysed during the simulation of the packer slug tests in the DFN model was the number of non-conductive intervals (NCIs) observed throughout the total length of the wells. From the core data, 624 fractures were observed in 288 m of core. Assuming that 20% of the fractures are conductive, 0.43 conductive fractures per meter were attained, on average. Therefore, an average 13 conductive fractures should be present in a 30-m simulated borehole. Assuming even fracture spacing, and 2-m-long packer intervals, ~3 NCIs should be expected in a 30-m-long packed borehole or 0.10 NCI/m. All of the model simulations showed a range of 0.14 to 0.17 NCI/m, suggesting that these DFN models conform reasonably well to field conditions. Any significant deviations are likely to be due to the sensitive relationship between the spacing of the horizontal beds and the length of the packer intervals. Whereas in the simulated model, the beds had constant spacing and were all considered conductive to some extent, in reality spacing showed considerable variation (and even a hint of bivariate spatial trends; Weiss et al. 2001; Weiss 2003) and not all of the beds were conductive.

As can be seen, the transmissivity generated by the DFN model and simulated wells can be modified using the size-transmissivity correlation coefficients to effectively condition the model to the field data. It should be noted that the transmissivity resulting from the

 DOI 10.1007/s10040-006-0039-y

horizontal beds was insensitive to changes in the correlation parameters. Similarly, the simulated transmissivity of the vertical fractures was insensitive to changes in transmissivity in the horizontal beds, allowing each of the curves to be calibrated separately to the field data.

Correlation-parameter maximization

The similar fits generated by different combinations of C_1 and C_2 reflect the non-uniqueness inherent to the parameter description. The simulated combinations, however, do allow for a determination of "envelopes" of probabilities for each of the parameter combinations. An elementary attempt was made to maximize the correlation-parameter estimates by calculating the difference (error) in the mean transmissivity values resulting from the model simulations and the field data. This error was then plotted against the two correlation parameters, as shown in Fig. 6, for each of the two conceptual models (multi-layer fractures with and without single-layer fractures; Fig. 4).

As can be seen, a distinct low line (trench) exists in each figure, representing the smallest differences between the simulated and actual mean values of log transmissivity. The deepest part of this "trench" in parameter space represents the best possible (albeit non-unique) combinations of the correlation parameters for proper calibration of the model to the transient field data. Each of the two conceptual models has its own unique (although similar) sets of correlation parameters. A comparison to the range of correlation parameters noted in the literature suggests that both models require especially low C_1 values to maintain a C_2 value within the range, as explained earlier. The discrepancy probably reflects (1) the difference between measured (large) mechanical apertures in controlled laboratory experiments (the basis of the literature values) and the significantly smaller effective hydraulic apertures derived from the field data, and to a lesser extent (2) the lithology other than chalk for which these parameters were determined (Table 1). It should be noted that hydraulic apertures can be orders of magnitude smaller than mechanical apertures due to mineral precipitation and crystallization, fault gouge, and typical roughness within discontinuity planes.

According to Fig. 6, model 2 (including single-layer fractures) appears to have correlation-parameter values closer to the literature range, thereby suggesting that it may be a more realistic model of the site. Again, however, the range of literature values may be a poor tool for measuring the validity of the models since the latter are based on actual field conditions. It appears that a more rigorous statistical technique is needed to help define the most appropriate values of C_1 and C_2 (perhaps the maximum relative entropy method; Woodbury et al. 1995; Woodbury and Ulrych 1998).

Conclusions

To better understand groundwater flow through the fractured Eocene chalk of the northern Negev, statistical data regarding fracture orientation, length (size) and intensity were obtained from 600 m of cores, 1,200 m of outcrops and 800 m of trenches dug into the saturated zone. This information was evaluated in combination with transmissivity values derived from packer slug tests. The transmissivity values obtained from the field tests could be reproduced after building the DFN model and simulating packer slug tests within a flow model based on an alternative approach to finite-element-type flow modelling. This reproduction of transient aquifer conditions is strong evidence that the model accurately represents site conditions. Although this information was collected at a specific field site, some of the observations can be generalized:

- Quantifying the percentage of hydraulically active fractures out of a total mapped fracture population is essential for a realistic modelling of flow in fractured rocks. At the northern Negev desert field site, only 13% of the overall mapped fractures proved to be active.
- Although in the literature the size distribution of multi-layer fractures is suggested to follow a power-law model, a lognormal distribution of size appeared to best describe both single-layer/short and multi-layer/long vertical fractures on site.
- For especially large fractures (multi-layer/long), neither the circular window nor the standard scanline techniques can capture the complete fracture size distribution. In particular, to characterize the spread of the fracture size data, larger-scale mapping methods combined with an as yet unavailable data-analysis technique need to be implemented.
- The observed bimodal distribution of transmissivity calculated from aquifer pumping tests may reflect the different discontinuity types existing in the rock (in this case study, the bedding planes and the vertical fractures).
- A conceptual DFN model which does not ignore the significance of single-layer vertical fractures may be more appropriate since the published fracture size-aperture data embedded in it provide a better fit.
- Finite-element, numerical models of DFNs have some difficulty reproducing the fine changes in hydraulic head observed from packed-off slug tests.
- A unique set of parameters that best represent a true correlation between fracture size and transmissivity should exist, and further work is needed to isolate the absolute values of the correlation coefficients that will provide the best fit to the data.

Acknowledgements We would like to thank Shimon (Bill) Dershowitz and Golder Associates for their help in running the DFN simulations using the FracWorks software. We would also like to thank the Ramat Hovav Regional Council for allowing us to roam the field site freely and for providing funding for this study. In addition, we thank the Kreitman School for Advanced

 DOI 10.1007/s10040-006-0039-y

Research and the Department of Geological and Environmental Sciences at Ben Gurion University of the Negev for their financial support.

References

Assaf L (2000) The hydraulic conductivity of the fracture systems intersecting the Avdat Group Chalk Ramat Hovav (in Hebrew), MSc thesis, Hebrew University of Jerusalem, Jerusalem

Bahat D (1991) Tectonofractography. Springer, Berlin Heidelberg New York

Bahat D (1999) Single-layer burial joints vs. single-layer uplift joints in Eocene chalk from the Beer Sheva syncline in Israel. J Struct Geol 21:293–303

Bahat D, Adar E (1993) Comment on "Analysis of subsurface flow and formation anisotropy in a fractured aquitard using transient water level data by B Rophe, B Berkowitz, M Margaritz and D Ronen". Water Resour Res 29(12):4171–4173

Bahat D, Shavit R (1997) Fracture in the Beer Sheva Syncline (Ramat Hovav). Report to the Ramat Hovav Industrial Municipality, Ramat Hovav, Israel

Bonnet E, Bour O, Odling NE, Davy P, Main I,Cowie P, Berkowitz B (2001) Scaling of fracture systems in geological media. Rev Geophys 39:347–381

Bouwer H (1989) The Bouwer and Rice slug test: an update. Ground Water 27:423–428

Bouwer H, Rice CR (1976) A slug test for determining hydraulic conductivity of unconfined aquifers with completely or partially penetrating wells. Water Resour Res 12:423–428

Cacas MC, Ledoux E, deMarsily G, Tillie B et al (1990) Modeling fracture flow with a stochastic discrete fracture network: calibration and validation. Water Resour Res 26(3):479–489

Cady CC, Silliman SE, Shaffern E (1993) Variation in aperture estimate ratios from hydraulic and tracer tests in a single fracture. Water Resour Res 29(9):2975–2982

Chiles JP, de Marsily G (1993) Flow and contaminant transport in fractured rock. Academic, New York, pp 169–236

Dershowitz W, Lee G, Geier J, Foxford T, LaPointe P, Thomas A (1998) FracMan interactive discrete feature data analysis geometric modeling and exploration simulation, User Documentation, Golder Associates, Seattle, WA

Dijk P, Berkowitz B, Bendel P (1999) Investigation of flow in water-saturated rock fractures using NMRI. Water Resour Res 35(2):347–360

Hatton CG, Main IG, Meredith PG (1994) Non-universal scaling of fracture length and opening displacement. Nature 367:160–162.

Johnston JD, McCaffrey KJW (1996) Fractal geometries of vein systems and the variation of scaling relationships with mechanism. J Struct Geol 18(2–3):349–358

Kurtzman D, Nativ R, Adar E (2003) Results from an intermediate-scale study area located at the confluence of the Naim and Hovav washes. In: Contaminant transport monitoring and remediation strategies in fractured chalk in the Northern Negev, FracFlux Project, Annual Report for the 2nd year, The Hebrew University of Jerusalem, Jerusalem, pp 69–82

LaPointe PR, Hudson JA (1985) Characterization and interpretation of rock mass joint patterns. Geol Soc Am Spec Pap 199

Long JCS, Doughty C, Datta-Gupta A, Hestir K, Vasco D (1998) Component characterization: an approach to fracture hydrogeology In: Dagan G and Neuman SP (eds) Subsurface flow and transport: a stochastic approach. International Hydrology Series, Cambridge University Press, New York

Main IG, Leonard T, Papasouliotis O, Hatton CG, Meredith PG (1999) One slope or two? Detecting statistically significant breaks of slope in geophysical data with application to fracture scaling relationships. Geophys Res Lett 26 (18):2801–2804

Mauldon M (1998) Estimating mean fracture trace length and density from observations in convex windows. Rock Mech Rock Eng 31(4):201–216

Nativ R, Nissim I (1992) Characterization of a desert aquitard: hydrologic and hydrochemical considerations. Ground Water 30 (4):598–606

Nativ R, Adar E, Dahan O, Geyh M (1995) Water percolation and solute transport through the vadose zone of fractured chalk under desert conditions. Water Resour Res 31:253–261

Nativ R, Adar E, Becker A (1999) Designing a monitoring network for contaminated groundwater in fractured chalk. Ground Water 37:38–47

Odling NE (1993) An investigation into the permeability of a 2D natural fracture pattern. Memoirs of the XXIVth Congress of IAA, IAA, ÅS, Norway

Odling NE (1997) Scaling and connectivity of joint systems in sandstones from western Norway. J Struct Geol 19(10): 1257–1271

Odling NE, Gillespie P, Bourgine B, Castaing C, Chiles J-P, Christensen NP, Fillion E, Genter A, Olsen C, Thrane, L Trice R, Aarseth E, Walsh JJ, Watterson J (1999) Variations in fracture system geometry and their implications for fluid flow in fractured hydrocarbon reservoirs. Petrol Geosci 5:373–384

Pollard DD, Segall P, Delaney PT (1982) Formation and interpretation of dilatant echelon cracks. Geol Soc Amer Bull 93:1291–1303

Priest SD, Hudson JA (1976) Discontinuity spacings in rock. Int J Rock Mech Min Sci Geomech Abstr 12:135–148

Renshaw CE, Park JC (1997) Effect of mechanical interactions on the scaling of fracture length and aperture. Nature 386: 482–484

Rophe B, Berkowitz B, Magaritz M, Ronen D (1992) Analysis of subsurface flow and formation anisotropy in a fractured aquitard using transient water level data. Water Resour Res 28(1):199–207

Rubin Y (2002) Applied stochastic hydrogeology. Oxford University Press, Oxford

Silliman SE (1989) An interpretation of the difference between aperture estimates derived from hydraulic and tracer tests in a single fracture. Water Resour Res 25(10):2275–2283

Stone D (1984) Sub-surface fracture maps predicted from borehole data; an example from the Eye-Dashwa Pluton, Atikokan, Canada. Int J Rock Mech Min Sci Geomech Abstr 21(4):183–194 (Abstract)

Stratford RG, Herbert AW, Jackson CP (1990) A parameter study of the influence of aperture variation on fracture flow and the consequences in a fracture network. In: Bartonand N and Stephansson O (eds) Rock joints, Balkema, Rotterdam, pp 413–431

Terzaghi RD (1965) Sources of error in joint surveys. Geotechnique 15:287–304

Tsang YW (1992) Usage of "Equivalent Apertures" for rock fractures as derived from hydraulic and tracer tests. Water Resour Res 28(5):1451–1455

Tsang YW, Tsang CF, Hale FV (1996) Tracer transport in a stochastic continuum model of fractured media. Water Resour Res 32(10):3077–3092

Vermilye JM, Scholz CH (1995) Relation between vein length and aperture. J Struct Geol 17(3):423–434

Villaescusa E, Brown ET (1992) Maximum likelihood estimation of joint size from trace length measurements. Rock Mech Rock Eng 25:67–87

Walmann T, Malthe-Sorenssen A, Feder J, Jossang T, Meakin P (1996) Scaling relations for the lengths and widths of fractures. Phys Rev Lett 77(27):5393–5396

Weisbrod N, Nativ R, Ronen D, Adar E (1998) On the variability of fracture surfaces in unsaturated chalk. Water Resour Res 34 (8):1881–1887

Weiss M (2003) Fracture and bedding plane control of ground water flow in a chalk aquitard; a geostatistical model from Israel. PhD thesis, Ben Gurion University, Beer Sheva, Israel

Weiss M, Rubin Y, Adar E (2001) Spatial distribution and characterization of fractures in the Negev site; a stochastic model. In: Contaminant transport monitoring and remediation strategies in fractured chalk in the northern Negev, FracFlux Project, Annual Report for the Year 2000, The Hebrew University of Jerusalem, Jerusalem

Woodbury AD, Ulrych TJ (1998) Minimum relative entropy and probabilistic inversion in groundwater hydrology. Stoch Hydrol Hydraul 12:317–358

Woodbury AD, Render F, Ulrych TJ (1995) Practical probabilistic ground water modelling. Ground Water 33(4):532–538

Zhang L, Einstein HH (1998) Estimating the mean trace length of rock discontinuities. Rock Mech Rock Eng 31 (4):217–235

Zimmerman DA, de Marsily G, Gotway CA, Marietta MG, Axness CL, Beauheim RL, Bras RL, Carrera J, Dagan G, Davies PB, Gallegos DP, Galli A, Gomez-Hernandez J, Grindrod P, Gutjhar AL, Kitanidis PK, Lavenue AM, McLaughlin D, Neuman SP, RamaRao BS, Ravenne C, Rubin Y (1998) A comparison of seven geostatistically based inverse approaches to estimate transmissivities for modeling advective transport by groundwater flow. Water Resour Res 34(6):1373–1413

 DOI 10.1007/s10040-006-0039-y